

rules out a spin assignment of 0 or 3 for the 3.58-Mev state (barring an attenuation of the coefficient in the spin 0 case). For spin 1 or 2, a dipole-quadrupole mixture is possible in the first transition. Figure 4 gives A_2 as a function of α^2 , the amount of mixing. The observed value of A_2 agrees with a spin assignment of 2 with $\alpha^2=0.075$ (0 phase) or ∞ , or with an assignment of 1 with $\alpha^2=0.12$ (π phase) or 8.0 (π phase). The elimination of a spin assignment of 0 or 3 for the state at 3.58 Mev is in agreement with conclusions^{1,2} reached from a consideration of intensities in the decay scheme in B¹⁰. In addition, the decay scheme favors the assign-

TABLE I. Theoretical values of A_2 in the expression $1+A_2 \cos^2\theta$.

	A_2		A_2
0(D)1(Q)3	-0.10	1(Q)1(Q)3	+0.05
1(D)1(Q)3	+0.05	2(Q)1(Q)3	-0.05
2(D)1(Q)3	-0.01	3(Q)1(Q)3	+0.02

ment of spin 2 rather than 1. If the spin is indeed known, then the correlation measurement provides a measure of the dipole-quadrupole mixture in the 2.86-Mev transition.

Nucleon Energy Levels in a Velocity-Dependent Potential*

A. A. ROSS,[†] R. D. LAWSON, AND HANS MARK[‡]

Department of Physics, University of California, Berkeley, California

(Received July 10, 1956)

The neutron and proton level sequences in a diffuse, velocity-dependent potential have been investigated. A velocity-dependent interaction is used which manifests itself by attributing to a nucleon inside nuclear matter an "effective mass" which is a function of its position. Following Brueckner, Johnson and Teller, and Duerr, the effective mass in the center of the nucleus is chosen to be one-half the free-particle mass. The potential form was taken as $V(r) = -V_0/\{1 + \exp[\alpha(r-a)]\}$, and for protons a Coulomb potential derived from a uniform charge distribution extending to $r=a$ was added. The proper neutron shell structure and level sequence was obtained with the parameters $\alpha = 1.16 \times 10^{13} \text{ cm}^{-1}$, $a = 1.3A^{1/3} \times 10^{-13} \text{ cm}$, $V_0 = 69 \text{ Mev}$, and a spin-orbit coupling 33 times the Thomas term. For protons, using the same α , radius, and spin-orbit coupling, it was found that the potential depth had to be increased by roughly 13 Mev to bind the correct number of protons in Pb²⁰⁸. If Pauli principle correlations are included, then a deeper proton potential is obtained. This correction depends critically on the form of the nucleon densities. Since a self-consistent treatment has not been made, this effect has been estimated in two ways: (1) A Fermi-Thomas approximation was used to compute the densities. In this case, the correct neutron-proton ratio is obtained but the correct proton level sequence is destroyed. (2) The neutron well depth was increased by an amount $(N + \frac{1}{2}Z)/(Z + \frac{1}{2}N)$. In this approximation the correct proton level sequence is obtained but it is not possible to bind the proper number of protons.

INTRODUCTION

THE phenomenological shell model of the nucleus proposed independently by Mayer and by Haxel, Jensen, and Suess¹ has achieved considerable success, particularly in explaining ground state properties of nuclei.² This might well be considered surprising in view of the strong two-body interactions exhibited, for example, in nucleon-nucleon scattering. Such forces would imply a strongly correlated wave function (indeed, if repulsive cores are introduced, the wave func-

tion must effectively vanish if two particles are sufficiently close) instead of a product of single-particle states. Further, the apparent short mean free path for collisions of nucleons in nuclei, indicated by the success of Bohr's compound nucleus model,³ also violates the idea of an independent-particle model. Indeed, for some time it was felt that a model in which the nucleons were pictured as moving in approximately independent orbits under the influence of a mean potential generated by the other nucleons in the nucleus, could not be at all successful.

However, once it was realized that a strong spin-orbit interaction would give reasonable results when taken in conjunction with a smooth average potential, the idea of a single-particle model was revived. It is well known⁴ that this average potential cannot arise from purely attractive Wigner-type forces since these

* Supported in part by the Office of Ordnance Research, U. S. Army.

[†] Whiting Fellow in Physics. Submitted in partial fulfillment of the requirements for the Ph.D. degree, University of California, Berkeley, California.

[‡] Now at the Radiation Laboratory, University of California, Livermore, California.

¹ M. G. Mayer, Phys. Rev. **75**, 1969 (1949); Haxel, Jensen, and Suess, Phys. Rev. **75**, 1766 (1949).

² See for example, M. G. Mayer and J. H. D. Jensen, *Elementary Theory of Nuclear Shell Structure* (John Wiley and Sons, Inc., New York, 1955).

³ N. Bohr, Nature **137**, 344 (1936).

⁴ See for example, J. M. Blatt and V. F. Weisskopf, *Theoretical Nuclear Physics* (John Wiley and Sons, Inc., New York, 1952).

do not lead to saturation. On the other hand, introducing two-body exchange forces is unsatisfactory since the condition for saturation gives more exchange than seems to be required to explain the two-body scattering data. Therefore, in order to obtain a total nuclear energy proportional to A (the mass number) and a radius proportional to $A^{1/3}$, one is essentially left with the need for repulsive and probably velocity-dependent forces which could be of either two-body or many-body character.⁵

Johnson and Teller⁶ have postulated the existence of a smooth shell-model-like nuclear potential, generated by a scalar meson field, and have examined under what conditions this can lead to saturation of nuclear forces. They find that if the potential is made velocity-dependent in such a way that within nuclear matter a nucleon moves as if it had a "reduced mass," then the experimentally observed saturation properties are reproduced. Further, according to their theory the spin-orbit interaction is larger than the usual Thomas term,⁷ and in heavy nuclei approximately the correct neutron-proton ratio is obtained. (This last result must be modified in view of further calculations described in this paper.)

This theory has been reformulated by Duerr⁸ in a relativistically invariant way which avoids the collapse of the nucleus at high momenta—a fault of the Johnson-Teller model. In Duerr's theory the nucleons are assumed to interact with an attractive scalar and a repulsive vector meson field. At normal densities the former gives a strong attraction and the latter a repulsion. However, at higher momenta the attraction decreases, leading to an over-all repulsion and hence to saturation. The potential experienced by a nucleon is the sum of the scalar and vector fields, both of which have a magnitude of several hundred Mev. On the other hand, the force exerted on an antinucleon is the difference of the scalar and vector interactions and consequently is very large. This has the interesting effect that the cross section for the interaction of an antinucleon with matter is considerably larger than that for a nucleon.^{8,9} This difference seems to be observed experimentally.¹⁰ Since the spin-orbit coupling arises through interactions in negative-energy states, a large antinucleon interaction implies a large spin-orbit coupling, as required by the shell model.

⁵ See for example, S. D. Drell and Kerson Huang, *Phys. Rev.* **91**, 1527 (1953), who have shown that in the perturbation limit the three-body forces derivable from pseudoscalar meson theory with pseudoscalar coupling are sufficient to give saturation.

⁶ M. H. Johnson and E. Teller, *Phys. Rev.* **98**, 783 (1955).

⁷ L. H. Thomas, *Nature* **117**, 514 (1926); D. R. Inglis, *Phys. Rev.* **50**, 783 (1936).

⁸ Hans-Peter Duerr, *Phys. Rev.* **103**, 469 (1956).

⁹ Hans-Peter Duerr and Edward Teller, *Phys. Rev.* **101**, 494 (1956).

¹⁰ Brabant, Cork, Horowitz, Moyer, Murray, Wallace, and Wentzel, *Phys. Rev.* **101**, 498 (1956); Chamberlain, Keller, Segrè, Steiner, Wiegand, and Ypsilantis, *Phys. Rev.* **102**, 1637 (1956).

On the other hand, Brueckner and his co-workers¹¹ have attempted to make a self-consistent nuclear model based on two-body interactions which give roughly the correct scattering up to 90 Mev. These potentials, which are derived from pseudoscalar meson theory neglecting the pair term,¹² lead to saturation because of their velocity dependence and nonmonotonic character. Despite the assumption of strong two-body forces, which means highly correlated wave functions, a transformation¹³ is introduced (equivalent to neglecting "incoherent scattering" on exclusion principle arguments) which, for an infinite nucleus, reduces the wave function to the product of plane waves moving in a dispersive medium. Since the scattering amplitudes have then to be evaluated in this medium, a self-consistent field problem arises. It is interesting to note that although these authors start from a completely different point of view than do Duerr or Johnson and Teller, they arrive at the same conclusion—namely that nucleons inside nuclear matter move as if they had an "effective mass" $m \approx 0.5m_0$, where m_0 is the mass of the free nucleon. (Note: m is defined throughout this work as the "effective mass.")

Although both the Duerr-Johnson-Teller and Brueckner theories lead to the study of a self-consistent field problem, these authors have neglected this and evaluated the constants of their theories in the Fermi-Thomas approximation. The purpose of this paper is not to consider the question of self-consistency but to take the simplest form of the single-particle equation (which is similar for all the above models) and see whether it is indeed possible to reproduce the shell-model level sequence. It should, therefore, be stressed that this work provides only (a) an affirmative answer to the question of whether the shell-model level sequence can be obtained with this type of velocity dependence and (b) eigenvalues and eigenfunctions which could be used as a starting point in making a self-consistent calculation.

WAVE EQUATION

The single-particle equation derivable from the Johnson-Teller Hamiltonian is

$$\left[\mathbf{p} \cdot \frac{1}{2m} \mathbf{p} + V(r) \right] \psi = E\psi, \quad (1)$$

where

$$m = m_0 / [1 + KV(r)]. \quad (2)$$

The value of K is chosen to approximately satisfy the saturation condition and $V(r)$ is, ideally, the self-

¹¹ Brueckner, Levinson, and Mahmoud, *Phys. Rev.* **95**, 217 (1954). K. A. Brueckner, *Phys. Rev.* **96**, 508 (1954); **97**, 1353 (1955). K. A. Brueckner and C. A. Levinson, *Phys. Rev.* **97**, 1344 (1955).

¹² K. A. Brueckner and K. M. Watson, *Phys. Rev.* **92**, 1023 (1953).

¹³ See for example, R. J. Eden and N. C. Francis, *Phys. Rev.* **97**, 1366 (1955) for a more detailed discussion of this type of approach.

consistent potential in which the particle moves. The spin-orbit interaction is taken to be the usual Thomas-type term multiplied by an appropriate constant, λ . Therefore, for neutrons the radial Schrödinger equation to be solved is

$$-\frac{\hbar^2}{2m_0} \frac{1}{r^2} \frac{d}{dr} \left[r^2 \left[1 + KV(r) \right] \frac{dR}{dr} \right] + \left(V(r) + \frac{\hbar^2}{2m_0} \frac{l(l+1)}{r^2} \left[1 + KV(r) \right] - \frac{\lambda \hbar^2}{4m_0^2 c^2} \frac{1}{r} \frac{dV}{dr} \left\{ \begin{matrix} l \\ -(l+1) \end{matrix} \right\} \right) R = ER, \quad (3)$$

where l is the orbital angular momentum of the particle, R is the radial wave function, and the operator $\sigma \cdot \mathbf{l}$ has been replaced by l and $-(l+1)$, its eigenvalues when operating on a state with $j=l+\frac{1}{2}$ and $j=l-\frac{1}{2}$ respectively.

Since a self-consistent treatment is not attempted, the Woods-Saxon¹⁴ form of the potential

$$V(r) = -V_0 / [1 + \exp \alpha(r-a)] \quad (4)$$

has been arbitrarily assumed. This has previously been investigated in connection with the static-shell-model level sequence.¹⁵

The level sequence obtainable from this type of interaction is a function of the five parameters K , V_0 , α , a , and λ . From considerations of the volume energy alone, Brueckner, Duerr, and Johnson and Teller arrive at the conclusion that the "effective mass" of a nucleon inside nuclear matter should be between 40% and 60% of the free nucleon mass. In view of this, K is chosen to be

$$K = -1/V_{0n}, \quad (5)$$

where V_{0n} is the neutron well depth. This implies that in the center of the nucleus a nucleon has a mass of approximately $0.5m_0$.

The well depth, V_{0n} , was chosen in such a way that the energy below the top of the well of the last filled level in Pb^{208} was roughly the same as in the static case.¹⁵ This allows comparison of the behavior of the uppermost levels in the static and velocity-dependent wells when they are "bound" by the same amount. When a self-consistent calculation is made, the energy below the top of the well is not necessarily equal to the experimentally observed separation energy, since in order to calculate the latter the change in energy of the meson field and the change in energy of the nucleons due to removal of one of them, must also be included.

The "nuclear radius" a was taken to be $a=r_0 A^{\frac{1}{3}}$, where r_0 was chosen to be 1.3×10^{-13} cm. This will lead to a radius of the charge distribution which is approxi-

mately 10% larger than obtained from high-energy electron scattering data.¹⁶ However, this was not felt to be important since the level sequence is invariant [i.e., Eq. (3) is invariant] under the transformation

$$\begin{aligned} V_0 r_0^2 &= V_0' r_0'^2, \\ \lambda V_0 &= \lambda' V_0', \\ \alpha r_0 &= \alpha' r_0', \\ KV_0 &= K' V_0', \\ r_0 r &= r_0' r', \\ Er_0^2 &= E' r_0'^2, \end{aligned} \quad (6)$$

and so the eigenvalues for other radii can easily be obtained.

Duerr's theory gives an expression for the spin-orbit coupling. However, the constants he derives are based on the approximation of an infinite nucleus, and hence may not be too reliable. The constant λ has, therefore, been kept as an open parameter. This constant, together with α , has been adjusted to give the observed shell-model level sequence for neutrons.

To study the proton level sequence the same α , λ , K , and r_0 were used. Further, it was assumed that the Coulomb potential a proton experiences is derivable from a uniform charge distribution extending out to $r=a$. This implies that for protons an additional potential

$$\begin{aligned} V_C(r) &= \frac{Z-1}{2a} e^2 \left[3 - \left(\frac{r}{a} \right)^2 \right] \quad \text{for } r < a \\ &= \frac{Z-1}{r} e^2 \quad \text{for } r > a \end{aligned} \quad (7)$$

must be added to Eq. (3).

Equation (3) can be readily solved in the limit that the potential is a square well. In this case, the solution for $r < a$ is, as in the static case ($K=0$), a spherical Bessel function with argument

$$[(2m/\hbar^2)(V_0-E)]^{\frac{1}{2}} r = [(m_0/\hbar^2)(V_0-E)]^{\frac{1}{2}} r.$$

For $r > a$, the solution is the same as in the static case, a spherical Hankel function of argument $(2m_0 E/\hbar^2)^{\frac{1}{2}} r$. The connection condition at $r=a$ is now

$$\begin{aligned} \frac{1}{m} \frac{dR}{dr} \Big|_{\text{inside}} &= \frac{1}{m_0} \frac{dR}{dr} \Big|_{\text{outside}} \\ &+ \frac{\lambda V_0}{4m_0^2 c^2} \frac{R(a)}{a} \left\{ \begin{matrix} l \\ -(l+1) \end{matrix} \right\}. \end{aligned} \quad (8)$$

From Eq. (8) it is seen that there is a finite discontinuity in the derivative of the wave function which arises from the form of the velocity dependence as well

¹⁴ R. D. Woods and D. S. Saxon, Phys. Rev. **95**, 577 (1954).

¹⁵ Ross, Mark, and Lawson, Phys. Rev. **102**, 1613 (1956).

¹⁶ Hahn, Ravenhall, and Hofstadter, Phys. Rev. **101**, 1131 (1956).

as the usual one due to the spin-orbit interaction. If the kinetic energy term in Eq. (3) had been taken as the non-Hermitian $(1/2m)\mathbf{p}^2$ rather than $\mathbf{p} \cdot (1/2m)\mathbf{p}$, then the connection condition at the nuclear radius would have been

$$\left. \frac{dR}{dr} \right|_{\text{inside}} = \left. \frac{dR}{dr} \right|_{\text{outside}} + \frac{\lambda V_0}{4m_0 c^2} \frac{R(a)}{a} (\ln 2) \left\{ \begin{matrix} l \\ -(l+1) \end{matrix} \right\}. \quad (9)$$

In the static case ($K=0$), the square well gave no shell at $N=126$ and led to an unsatisfactory level sequence. In the velocity-dependent case the results are considerably worse. The high angular momentum states, which were already too tightly bound, are now pulled down even further. This can be seen as follows: The connection condition, Eq. (9), is essentially the same as the condition in the static case except that the spin-orbit coupling is changed and that $(V-E)$ in the argument of the interior wave function is changed to $(V-E)/2$. This means that if two levels with different angular momenta are bound by the same energy in the static potential, they will still be bound by the same energy in the velocity-dependent well if $(\ln 2)(\lambda V_0)_{\text{vel. dep.}} = (\lambda V_0)_{\text{static}}$. The spacing between all levels will be roughly doubled provided the same number of levels are bound, since $V_{\text{vel. dep.}} \approx 2V_{\text{static}}$. Therefore, if an equation with a kinetic energy term $(1/2m)\mathbf{p}^2$ is used, no great violence is done to the level sequence.

On the other hand, the operator $\mathbf{p} \cdot (1/2m)\mathbf{p}$, which has been used, gives rise to a term $K(dV/dr)(dR/dr)$ in the radial equation. This term is responsible for the additional discontinuity in the wave function and is the major cause for the disrupted level sequence. In the square-well limit, this term gives rise to a δ -function attraction since $(1/R)(dR/dr)$ must always be negative at the radius of the potential for a bound level. Furthermore, the term is likely to be more important for levels with large angular momenta and few radial nodes since for these the wave function is larger at the edge. As an example of this effect consider the behavior of the $3s$ and $1h$ levels in Ce^{140} neglecting spin-orbit coupling (i.e., $\lambda=0$). In the static case with $V_0=42.8$ Mev, the $3s$ level is bound by 10.94 Mev and the $1h$ state is above it at 10.73 Mev. Using Eq. (9) with $V_0=72$ Mev, the $3s$ level is at 8.79 Mev and the $1h$ level is above it at 8.43 Mev. If the matching condition, Eq. (8) is used, then the $3s$ level is pulled down to 12.23 Mev and the $1h$ level is at 14.62 Mev. In addition, if the spin-orbit coupling (with $\lambda=39.5$) is included, the center of gravity of the $1h_{9/2}$ and $1h_{11/2}$ levels using Eq. (9) is depressed by 1.95 Mev and the two levels are split by 13.1 Mev, whereas with Eq. (8) the center of gravity descends 2.30 Mev and the splitting of the levels is 14.0 Mev.

The foregoing discussion of the square-well limit suggests that it may be necessary to use a somewhat smaller λ and a larger potential surface thickness than was necessary in the static well to obtain the correct level sequence.

The differential analyzer at UCRL was programed to study the eigenvalue problem. Methods exactly analogous to those described previously¹⁵ were used to find solutions. As in that case, the errors introduced by the boundary condition approximations were considerably less than those inherent in the machine. In absolute magnitude the latter were increased, over the static case, by the doubling of the energy scale and the necessary use of two input plots—one of the potential and one of the effective mass. The eigenvalues quoted here are accurate to approximately 0.2 Mev in relative spacings. The absolute magnitude is probably a little less accurate.

RESULTS

(a) Neutrons

For the purpose of comparison and orientation, the top levels in various nuclei were first investigated with the parameters that were optimum in the static case, $\alpha=1.45 \times 10^{13}$ cm⁻¹, $\lambda=39.5$, $r_0=1.3 \times 10^{-13}$ cm. The well depth, V_{0n} , was taken to be 72 Mev, which gives a "binding" of 7.9 Mev for the $3p_{1/2}$ level in Pb^{208} . The results are shown in Fig. 1.

It can be seen that although the situation is very greatly improved from the square-well limit—a shell is obtained at $N=126$ and the high angular momentum levels have been raised—it is by no means ideal and

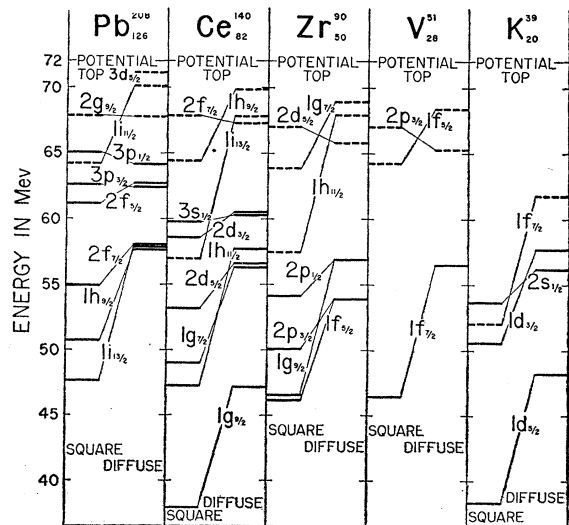


FIG. 1. Top neutron levels in nuclei with $N=20, 28, 50, 82,$ and 126 . The parameters used to determine the energy levels in the diffuse potential are: $\alpha=1.45 \times 10^{13}$ cm⁻¹, $V_0=72$ Mev, $a=1.34 \times 10^{-13}$ cm, and $\lambda=39.5$; $m_{\text{eff}}=0.5m_0$ at $r=0$. The square-well level sequences for the same values of $V_0, a,$ and λ are also shown. The dotted lines indicate unfilled levels in both the square and the diffuse potential.

does not yet display the satisfactory characteristics obtained in the static case. The high angular momentum states are still somewhat too tightly bound. For example, the $1h_{11/2}$ level lies too low in the well and this would have the consequence that the ground state configurations beyond $N=64$ would be either $1h_{11/2}$ or allowing for pairing, possibly $2d_{5/2}$ or $1g_{7/2}$, which is not observed.

Since the $3s_{1/2}$ level fills in together with the $1h_{11/2}$, these two levels should lie approximately at the same energy. Similarly, the $1g_{9/2}$ level should probably lie above the $2p_{1/2}$ since the last three odd neutron nuclei before the $N=50$ shell, Sr^{87} , Kr^{88} , and Se^{79} all have spins consistent with a $1g_{9/2}$ configuration. Finally, in K^{39} the $2s_{1/2}$ and the $1d_{5/2}$ levels are split by 8 Mev whereas the shell spacing between the $2d_{3/2}$ and the $1f_{7/2}$ is only 4.1 Mev, so that a strong shell should appear at $N=14$ rather than at $N=20$. In view of these considerations it is apparent that both α and λ must be changed.

In order to find a more suitable set of potential parameters, the behavior of several representative energy levels was investigated as the surface thickness Δ was varied. [The surface thickness, Δ , is defined as the distance from the point where the potential has 90% of its maximum value to the point where it has 10%, $\Delta = (2 \ln 9)/\alpha$.]

It was demonstrated in the static case that treating

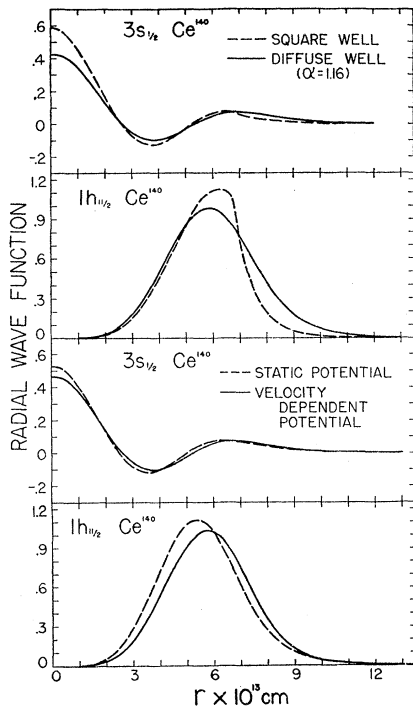


FIG. 2. The upper panels show the wave functions of the $3s_{1/2}$ and $1h_{11/2}$ levels in a square and a diffuse ($\alpha=1.16 \times 10^{13} \text{ cm}^{-1}$) velocity dependent potential. The lower panels compare the wave functions of the same levels in a static and velocity-dependent potential, both with $\alpha=1.45 \times 10^{13} \text{ cm}^{-1}$.

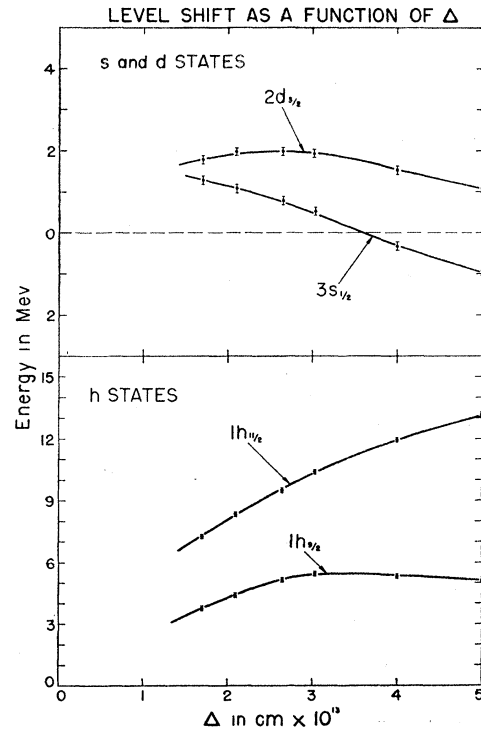


FIG. 3. The energy shift of four representative levels as the surface layer of the potential is increased is shown in this figure. The points indicate the magnitude of the errors in the eigenvalues determined with the differential analyzer. These calculations are made with $V_0=72 \text{ Mev}$, $\lambda=39.5$, and $\alpha=1.34 \times 10^{13} \text{ cm}^{-1}$.

the potential slope by first-order perturbation theory was quite inadequate for quantitative estimates. The introduction of a velocity dependence increases the dependence of the wave function on the surface thickness, Δ . This can be seen in Fig. 2. Thus first-order perturbation theory is of even less use than in the static case for estimating the behavior of energy levels when the surface thickness is varied.

In Fig. 2 there is also a direct comparison between the wave functions in the velocity-dependent and static cases for a surface thickness, $\Delta=3.03 \times 10^{13} \text{ cm}$. It may be seen that the wave functions in the former case reach their last maxima at larger values of r than in the latter case. This is so because in the velocity-dependent case the nucleon mass is closer to m_0 for $r > a$ than for $r < a$ and the "effective potential," mV , thus becomes more important for large r . The effect may also be regarded as an increase of $(\ln 2)/\alpha$ in the "effective" nuclear radius of the "effective potential." This increase in the radius obviously tends to increase the binding energies of the levels with increasing Δ which opposes the usual effects tending to raise levels, and in fact overcomes them for large values of Δ . (See the $3s_{1/2}$, $2d_{3/2}$, and $1h_{9/2}$ levels shown in Fig. 3.)

However, as far as the relative shift of levels of different angular momenta is concerned, the general behavior is similar to the static case: As the thickness

of the surface increases, the higher angular momentum levels shift upwards in the well relative to those of lower angular momentum. The more tightly bound a level, and the fewer nodes it has, the more rapid is the shift as Δ changes. Also, for a fixed value of Δ , levels of total angular momentum $j=l+\frac{1}{2}$ move downwards and of $j=l-\frac{1}{2}$ move upwards when λ is increased, and the magnitude of the splitting of two such levels is roughly proportional to the orbital angular momentum, l .

There are two other effects, which like the increase in the "effective" radius, tend to obscure rather than alter the behavior of the energy of levels with changing Δ . First, the derivative at the origin of the curves shown in Fig. 3 is negative, although it very rapidly becomes positive. Intuitively this can be seen in the limit from the "effective potential" argument given above. Alternatively, it can be rigorously derived in the limit from the equation

$$\frac{dE_{\Delta}}{d\Delta} = -\frac{dE_B}{d\Delta} = -\int_0^{\infty} R^2 \frac{dH}{d\Delta} r^2 dr, \quad (10)$$

where R is the radial wave function, E_B is the binding energy in the diffuse potential, and E_{Δ} ("binding energy" in square well) - ("binding energy" in diffuse well). In the limit that $\Delta \rightarrow 0$, this leads to

$$\frac{dE_{\Delta}}{d\Delta} = -\frac{\ln 2}{2 \ln 9} a^2 R^2(a) \left[\frac{1}{2} V_0 - \frac{1}{2} E_B \right]. \quad (11)$$

Equation (11) yields a negative slope of $\sim(-0.9)$ for the $3s_{1/2}$ level and $\sim(-5.1)$ for the $1h_{11/2}$. These slopes are omitted from Fig. 3 because it is difficult to determine eigenvalues on the machine in the region of small Δ owing to the sharpness of the potential edge. Furthermore, this region is of little interest from the point of view of obtaining good level sequences. However, Eq. (10) provides a very useful check on the $3s_{1/2}$ level curve in Fig. 3 since the machine eigenvalues are not accurate enough to distinguish the shape without the aid of a calculated derivative.

Second, the magnitude of the spin-orbit splitting, for fixed λ , decreases with increasing Δ . The splitting of the $1h_{11/2}$ and $1h_{9/2}$ levels in Ce^{140} for $\lambda=39.5$ decreases from 14.1 Mev for $\Delta=0$ to 9.1 Mev at $\Delta=5 \times 10^{-13}$ cm, which is less than two-thirds of its original value. This can be considered partially as a consequence of the effective doubling of the spin-orbit term outside the nuclear radius and partially as a consequence of the decrease in magnitude of the wave function near the nuclear radius as Δ is increased (see Fig. 3). Despite this, for fixed Δ in the region of interest, one can roughly take the spin-orbit splitting as proportional to λ and the two levels as having a fixed center of gravity.

Bearing all these facts in mind, plus the fact that the lighter the nucleus the farther a given angular mo-

mentum level is shifted when Δ is changed,¹⁷ it is possible to make rough predictions about the positions of levels for a given Δ and λ in the region of interest. The most critical region for choosing the parameters α and λ is again near the 82 shell where the $3s_{1/2}$, $2d_{3/2}$, and $1h_{11/2}$ levels are all in competition. From single-particle assignments² it is clear that the $2d_{3/2}$ and the $1h_{11/2}$ levels must lie above the $3s_{1/2}$ level. The requirement that the $1h_{11/2}$ level lie between the $3s_{1/2}$ and $2d_{3/2}$ levels (as in the static case) is unnecessarily stringent since the $1h_{11/2}$ state, due to its high angular momentum fills in pairs with appreciable pairing energy.¹⁸ It has, therefore, been allowed to lie slightly above the $2d_{3/2}$ level. In order to raise the $1h_{11/2}$ level relative to the other two levels, it is necessary to decrease λ , increase Δ , or to do both. Making the restriction that the $2d_{3/2}$ level lies above the $3s_{1/2}$ level and at the same time minimizing both λ and the surface thickness, the following "final" parameters¹⁹ are obtained: $\lambda=33$, $\alpha=1.16 \times 10^{13}$ cm⁻¹, and $V_{0n}=69$ Mev. (The well depth was chosen to bind the $3p_{1/2}$ level in Pb^{208} by approximately 7.4 Mev.)

The purpose of trying to keep both α and λ minimal is to obtain as close agreement as possible with the electron scattering measurements of the surface thickness, and Duerr's prediction for the magnitude of the spin-orbit interaction. Also it is not desirable to exaggerate the crossovers of the $2f_{7/2}$ and $1h_{9/2}$ levels, the $2d_{5/2}$ and $1g_{7/2}$ levels, and the $2p_{3/2}$ and $1f_{5/2}$ levels. These crossovers would be increased by an increase in either Δ or λ . If for neutrons the $2f_{7/2}$ level is too much more tightly bound than the $1h_{9/2}$ level, then it cannot be expected that the correct level sequence will be obtained for protons since, in the proton case, the $1h_{9/2}$ level must lie below the $2f_{7/2}$ state to give the right spin and parity for the ground state of Bi^{209} .

In the region $N=50$ to 64, it is not certain that the $2d_{5/2}$ level lies much below the $1g_{7/2}$ since these levels fill in together. In addition, from the ground state spins of Cr^{53} and Fe^{57} , the $2p_{3/2}$ level is assigned to lie below the $1f_{5/2}$, but the spacing between these levels should be considerably smaller than the shell spacing.

It can be seen from Fig. 4 that very good agreement with assignments from ground state spins and parities is indeed obtained with these parameters, except in the region in the middle of the $N=82$ to $N=126$ shell, which is for neutrons the region of strong distortion. Some criticism might perhaps be made of the spacings of levels. For example the $1g_{9/2}$ level now lies correctly above the $2p_{1/2}$ level, but in Zr^{90} it is 2.4 Mev above it.

¹⁷ The $1i$ states in Pb^{208} , for example, behave, as in the static case, remarkably like the $1h$ states in Ce^{140} and the $1g$ states in Zr^{90} , etc.

¹⁸ R. D. Lawson and A. A. Ross, Bull. Am. Phys. Soc. Ser. II, 1, 246 (1956).

¹⁹ α could actually be very slightly larger if the $1h_{11/2}$ state returned to its previous position between the $2d_{3/2}$ and $3s_{1/2}$ levels. The latter are so close, however, that it is not possible to quote more exact minimum values.

In view of the assignment $2p_{1/2}$ to Se^{77} as well as to Zn^{69} , this seems large. Similarly, in V^{51} the unfilled $2p_{3/2}$ and $1f_{5/2}$ levels are split by 2.6 Mev. Other levels which might properly be closer together show similar wide spacings.

However, two things should be remembered. In the first place the large splitting of the $2p_{3/2}$ and $1f_{5/2}$ levels in V^{51} does not persist as more nucleons are added (in Zr^{90} these levels are only split by 0.2 Mev) and hence when the $2p_{3/2}$ and $1f_{5/2}$ particles start to fill in, it is likely that the energy difference between these levels is less than 2.6 Mev. Secondly, all level spacings are roughly doubled since the well depth is roughly doubled. This circumstance is indeed desirable from the point of view of explaining the frequencies encountered in the nuclear photoeffect.²⁰

The shells occur at the proper places with spacings of about 6 Mev and hence are unmistakable. The overall conclusion is that a satisfactory neutron shell structure and level sequence can be obtained for a velocity-dependent potential of this type.

(b) Protons

In the static case it is well known that the same nuclear potential will not bind the correct number of neutrons and protons. This can be seen, in the square-well limit, by a Fermi-Thomas argument, showing that the difference between the maximum kinetic energies of the correct numbers of neutrons and protons is only just over one-half the height of the Coulomb potential at the radius of the nucleus. As has been pointed out by

McMillan,²¹ it may also be seen from the symmetry energy term in the semiempirical mass formula.²² On the other hand, a Fermi-Thomas estimate for a square well in which one decreases the effective mass of a nucleon to approximately one-half of its free value indicates that in this case the same nuclear well will bind the correct number of neutrons and protons.⁶ However, as soon as the sides of the well are sloped, the protons not only move in a well which is shallower because of the Coulomb potential, but also one which has a smaller radius. They are restricted to a smaller volume than the neutrons²³ and therefore it is still necessary to increase the proton nuclear well depth. In fact it was found in Pb^{208} that, to obtain comparable binding for top neutron and proton levels, it was necessary to choose a proton well depth roughly 12 Mev deeper than the neutron well depth. In the static case a difference of 14 Mev was necessary, which is, of course, proportionally larger since the well depth for neutrons was then only 42.8 Mev. In the static case, this increase was also greater than estimated by a Fermi-Thomas calculation.

That the neutron and proton well depths are different is perhaps not too surprising in view of the fact that throughout all these considerations the exclusion principle has been neglected. One can crudely estimate the effect of the Pauli correlations by assuming that in the vicinity of a nucleon half of the like nucleons are sufficiently excluded (since half will have parallel spin) to give no contribution to the force field. Since in a heavy nucleus there are more neutrons than protons, this would provide a deeper well for protons. Taking this quite literally gives for the proton potential

$$V_p(r) = V_n(r) \left[\frac{\rho_n(r) + \frac{1}{2}\rho_p(r)}{\rho_p(r) + \frac{1}{2}\rho_n(r)} \right], \quad (12)$$

where V_n is an appropriately chosen neutron well, and $\rho_n(r)$ and $\rho_p(r)$ are, respectively, the neutron and proton radial density distributions.

The factor one-half appearing in this argument is certainly an upper limit on the exclusion effect since it is based on the assumption that the nucleon is essentially a δ -function source for the meson field.²⁴ The exclusion effect is, of course, properly handled by introducing nucleon densities derived from antisymmetrized wave functions into the Duerr-Johnson-Teller field equations. However, it is hoped that some idea of the magnitude of the effect can be obtained from Eq. (12).

In general, if Eq. (12) is used, the top proton level is sufficiently bound compared to the top neutron,

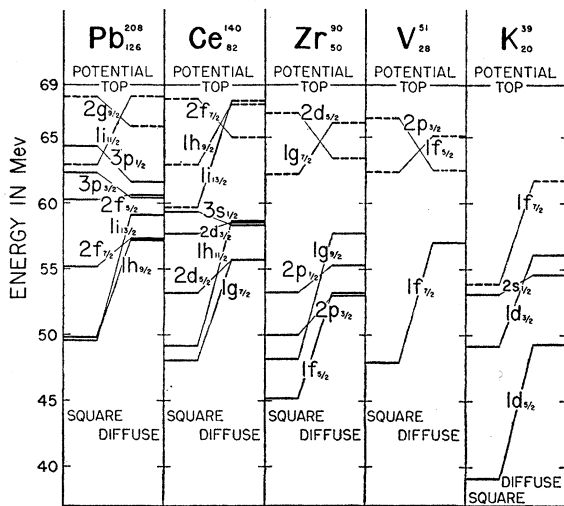


FIG. 4. Top neutron levels in nuclei with $N=20, 28, 50, 82,$ and 126 . The parameters used to determine the energy levels in the diffuse potential are: $\alpha=1.16 \times 10^{13} \text{ cm}^{-1}$, $V_0=69 \text{ Mev}$, $a=1.34 \times 10^{-13} \text{ cm}$, and $\lambda=33$; $m_{\text{eff}}=0.5m_0$ at $r=0$. The square-well level sequences for the same values of $V_0, a,$ and λ are shown. Dotted lines indicate unfilled levels in both the square and the diffuse potential.

²⁰ S. Rand, Phys. Rev. **99**, 1620 (1955).

²¹ W. G. McMillan, Phys. Rev. **92**, 210 (1953).

²² N. Bohr and J. A. Wheeler, Phys. Rev. **56**, 426 (1939); E. Fermi, Nuclear Physics (University of Chicago Press, Chicago, 1950); A. E. S. Green, Phys. Rev. **95**, 1006 (1954).

²³ M. H. Johnson and E. Teller, Phys. Rev. **93**, 357 (1954).

²⁴ This assumption also violates the contention that the meson field is classical, since under these conditions the quantum fluctuations are not obviously small.

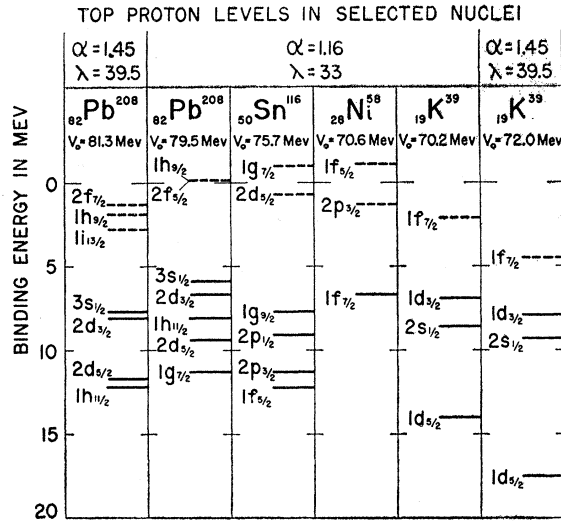


FIG. 5. Top proton levels in selected nuclei. The top proton levels in K^{39} , Ni^{58} , Sn^{116} , and Pb^{208} are shown for the parameters $\alpha = 1.16 \times 10^{13} \text{ cm}^{-1}$, $a = 1.34 \times 10^{-13} \text{ cm}$, and $\lambda = 33$. The well depths have been adjusted according to Eq. (13) in the text. The top proton levels in Pb^{208} and K^{39} for the parameters $\alpha = 1.45 \times 10^{13} \text{ cm}^{-1}$, $a = 1.34 \times 10^{-13} \text{ cm}$, and $\lambda = 39.5$ are also shown. The well depths have been arbitrarily adjusted to bind the proper number of protons. Dotted lines indicate unfilled levels.

since in addition to an over-all increase in depth, the proton potential also has a larger effective radius than the neutron potential. This follows because the proton density has less radial extent than the neutron density when the potential radius is the same. Such a proton potential appears also, in first approximation, to give a characteristically unsatisfactory level sequence. This latter effect arises because, compared to the neutron density distribution, that of the protons has a hole at the center and a steeper slope, both effects being due to the additional Coulomb potential. Thus the proton potential is depressed at $r=0$ and has a larger surface layer. This shape tends to undo the desirable effect of the Coulomb potential which, for example, in the static case reversed the ordering of the proton $3s_{1/2}$ and $2d_{3/2}$ levels compared to the neutron ordering. If the densities obtained in the static case¹⁵ for Au^{197} are used to calculate the proton potential according to Eq. (12), the above-mentioned effects obviously lead to a potential of hopeless shape. These effects are less pronounced but still present even if the Fermi-Thomas approximation for the densities is used. Assuming Eq. (12) and a Fermi-Thomas nucleon distribution, the last filled proton level in Pb^{208} is bound by approximately 1 Mev more than the last neutron level, but the $1h_{9/2}$ and $2f_{7/2}$ levels appear in the wrong order. The full understanding of this situation requires a self-consistent field calculation.

For the present purpose, it has been assumed that ρ_n and ρ_p inside the nucleus are constant and that both drop to zero simultaneously. Equation (12) can then

be rewritten as

$$V_p(r) = V_n(r)(N + \frac{1}{2}Z)/(Z + \frac{1}{2}N), \quad (13)$$

where N and Z are the number of neutrons and protons respectively in the nucleus. For convenience we have used Eq. (13) in adjusting the depth of the proton potential. Such a well does not bind quite the proper number of particles since the radius is no longer enlarged. It gives, however, a level sequence in close agreement with experiment. The results obtained when the proton well is adjusted according to Eq. (13) are shown in Fig. 5. Where levels of interest are outside the well, they are shown by extrapolating from their positions in a deeper well. The value of K , though chosen arbitrarily in this work, is in principle determined from saturation conditions. Therefore, it is taken to be the same for neutrons and protons, which implies a smaller effective mass for protons than for neutrons.

From Fig. 5 it is seen that good shell structure and a reasonably satisfactory level sequence are obtained on the basis of the above assumptions. For example, the required crossover of the $2d_{3/2}$ and $3s_{1/2}$ levels has occurred. On the other hand, the $1h_{9/2}$ level is actually 0.1 Mev less tightly bound than the $2f_{7/2}$ level.²⁵ This is close enough so that if a self-consistent Coulomb potential were used, it is probable that the desired crossover would occur, thus giving the correct assignment of $1h_{9/2}$ for the ground state of Bi^{209} .

It has already been remarked that the surface thickness of the potential has to be chosen approximately $0.8 \times 10^{-13} \text{ cm}$ greater than in the static case in order to achieve the same level ordering. It would be of interest to know whether this is likely to bring the proton density into closer agreement with results from the high-energy electron scattering experiments¹⁶ which give a radius of $(1.07 \pm 0.02) \times 10^{-13} \text{ cm}$ and a surface thickness roughly constant for all A and equal to $(2.4 \pm 0.3) \times 10^{-13} \text{ cm}$. In the static case the quantities

$$\rho_n(r) = \text{const} \left(\frac{2m_0[V_n(r) - E_B]}{\hbar^2} \right)^{\frac{3}{2}} \quad \text{and} \quad \rho_p(r) = \text{const} \left(\frac{2m_0[V_p(r) - V_C(r) - E_B]}{\hbar^2} \right)^{\frac{3}{2}}, \quad (14)$$

where E_B is the "binding energy" of the last bound level, gave a reasonable estimate of the actual densities.¹⁵ In this case we have made an estimate, replacing m_0 by m . It is less certain how accurate this is since it does not distinguish between the different forms of Eq. (3), that is, the approximation does not distinguish between the equation with $(1/2m)\mathbf{p}^2$ and $\mathbf{p} \cdot (1/2m)\mathbf{p}$. However, the changes in the wave functions from the static case are not too drastic and hence it is probable that an estimate based on Eq. (14) with m_0 replaced by

²⁵ This is really a smaller spacing than our accuracy can determine.

m , will not be too unreasonable. According to this, the proton distributions in Pb^{208} and Sn^{116} have radii of 7.56×10^{-13} cm ($r_0 = 1.276 \times 10^{-13} A^{\frac{1}{3}}$) and 6.05×10^{-13} cm ($r_0 = 1.241 \times 10^{-13} A^{\frac{1}{3}}$), and surface thicknesses of 2.28×10^{-13} cm and 2.36×10^{-13} cm respectively. The difference in these two results is due partly to the difference in "binding energies" of the top levels (7.33 Mev in Pb^{208} and 6.1 Mev for Sn^{116}) and partly to the difference in the Coulomb potential. The increase in the radii compared to the static case is mainly a consequence of the difference in the radii of the potential and the "effective potential," which has already been pointed out. Although these radii are larger than the values obtained from high-energy electron scattering,¹⁶ they could easily be remedied without impairing the level sequence by choosing a smaller initial potential radius, r_0 . On the other hand, the surface thicknesses compare quite favorably with the experimental results.

COMPARISON WITH DUERR'S MODEL

In this section we wish to examine the effect of using Duerr's⁸ relativistically invariant formulation of the Johnson-Teller model. For this purpose we shall look at the nonrelativistic limit of Duerr's Dirac Hamiltonian for the nucleon, and try to estimate how much change would be introduced in the results quoted in this paper by the use of his equations. Using the Foldy-Wouthuysen transformation,²⁶ Duerr shows that his Hamiltonian reduces to

$$\begin{aligned} & \frac{1}{8m_0} \left[\mathbf{p} \cdot \frac{2}{1-a\phi} \mathbf{p} + \mathbf{p}^2 \frac{1}{1-a\phi} + \frac{1}{1-a\phi} \mathbf{p}^2 \right] \psi \\ & - [am_0\phi - bm_0\phi_0] \psi + \frac{1}{8m_0} \nabla \cdot \left[\frac{\nabla b\phi_0}{(1-a\phi)^2} \right] \psi \\ & + \frac{1}{4m(1-a\phi)^2} \boldsymbol{\sigma} \cdot [\nabla(a\phi + b\phi_0) \times \mathbf{p}] \psi = 0, \quad (15) \end{aligned}$$

where \hbar and c have been set equal to unity,²⁷ ϕ and ϕ_0 are the scalar and vector meson fields respectively, and a and b are constants which determine the strengths of these fields. The term $[bm_0\phi_0 - am_0\phi]$ corresponds to the mean potential $V(r)$. The last term in the equation gives the spin-orbit coupling. The term containing ∇^2 operating on ϕ and ϕ_0 has been omitted in the Hamiltonian considered in our paper.

The simplest assumption to make is that the two fields ϕ and ϕ_0 have the same radial dependence. This is obviously not necessary but no direct information is available about this, since Duerr neglects gradient terms which give information on the meson masses. It

²⁶ L. L. Foldy and S. A. Wouthuysen, Phys. Rev. **78**, 29 (1950).

²⁷ It should be noted that if the symmetrized form of the operator $\mathbf{p}^2/2m$ had been taken, Eq. (3) would have contained three terms similar to the first three terms in Eq. (15). See for example H. Weyl, *Gruppentheorie und Quantenmechanik* (Verlag Von S. Hirzel, Leipzig, 1928).

has therefore been assumed that both fields have the same radial dependence:

$$\begin{aligned} m_0 a \phi &= -\frac{V_1}{1 + \exp[\alpha(r-a)]} \quad \text{and} \\ m_0 b \phi_0 &= \frac{V_2}{1 + \exp[\alpha(r-a)]}. \quad (16) \end{aligned}$$

In view of the large surface thickness of the potential, Duerr's values for $a\phi$ and $b\phi_0$ shall not be used since these numbers would probably not be the same if surface terms had been included in his calculations. Instead, it shall be required that the sum of the fields (16) be 69 Mev, the neutron well depth, and that the effective mass of a nucleon at $r=0$ be $0.5m_0$ (which, in Duerr's theory means that $a\phi=0.5$ at $r=0$). The constants in (16) then become $V_1=469.75$ Mev and $V_2=400.75$ Mev.

If we define $f=m_0/m$, then $8m_0$ times the "kinetic energy" operator in Eq. (15) becomes

$$\begin{aligned} & 2\mathbf{p} \cdot f\mathbf{p} + \mathbf{p}^2 f + f\mathbf{p}^2 \\ & = 2\mathbf{p} \cdot f\mathbf{p} + \mathbf{p} \cdot f\mathbf{p} + \mathbf{p} \cdot [\mathbf{p}, f] + \mathbf{p} \cdot f\mathbf{p} + [f, \mathbf{p}] \cdot \mathbf{p} \\ & = 4\mathbf{p} \cdot f\mathbf{p} - \hbar^2 \nabla^2 f. \quad (17) \end{aligned}$$

Thus when the Hermitian form is taken in a symmetrized manner, a small correction which is effectively a contribution of $(\hbar^2/8m_0)\nabla^2 f$ to the potential well depth is introduced:

$$\frac{\hbar^2}{8m_0} \nabla^2 f = \frac{\hbar^2}{8m_0} \left[\frac{2f'}{r} + f'' \right]. \quad (18)$$

The first term in this equation is similar to the spin-orbit term (forgetting temporarily the changed form of the effective mass which we shall consider presently) but acts equally on all energy levels. For the surface thickness considered here, $\Delta \sim 3.8 \times 10^{-13}$ cm, this should have little relative effect between different levels, but add an energy $(mc^2/\lambda V_0)[1/(2l+1)] \times$ (spin-orbit splitting of levels) to each energy level. For the h states in Ce^{140} this amounts to approximately 0.33 Mev and for the d states to 0.24 Mev, which does indeed appear negligible. The second term makes the slope of the potential appear slightly less sharp since f'' is negative inside the nuclear radius and positive outside. The change is very small and for $\alpha=1.16 \times 10^{-13}$ cm it leads to an apparent increase in Δ of $\sim 0.1 \times 10^{-13}$ cm.

On the other hand, the extra term

$$\begin{aligned} & \frac{1}{8m_0} \nabla \cdot \left[\frac{\nabla b\phi_0}{(1-a\phi)^2} \right] \approx \frac{1}{16m_0} \nabla \cdot f^2 \nabla f \\ & = \frac{1}{2m_0} \left[\frac{f^2}{4} f'' + \frac{f^2 f'}{4r} + \frac{f(f')^2}{4} \right] \quad (19) \end{aligned}$$

has the opposite effect from Eq. (18) since all terms are

of opposite sign. Inside the nucleus it is of the same magnitude as Eq. (18) and hence we can roughly neglect the sum of all these terms.

Of far larger consequence is the change in form of the effective mass itself. If the constants in the two formulations are chosen to give the same effective mass both inside and outside nuclear matter, the effective mass will still have a considerably different value in the surface region in the two cases. In the Duerr formulation, the effective mass is

$$m_D = (1 - a\phi)m_0 = \left(1 + \frac{1}{2} \frac{V(r)}{V_0}\right) m_0 \quad \text{for} \\ m = 0.5m_0 \quad \text{at} \quad r = 0,$$

whereas throughout this work an effective mass defined by Eqs. (6) and (5) has been used. Thus by definition, for all r , $m_D > m$ (e.g., at the nuclear radius $m_D = \frac{3}{4}m_0$ whereas $m = \frac{2}{3}m_0$). Consequently, the "effective potential," mV , in Duerr's case for the same $V(r)$ is actually greater. One can get a rough estimate of this effect by examining the change in the "effective potential":

$$V_{\text{eff}}^D(r) = m_D(r)V(r), \\ V_{\text{eff}}^{JT}(r) = m(r)V(r).$$

Duerr's effective potential extends 0.167Δ , 0.053Δ , and 0.018Δ further out at $9/10$, $1/2$, and $1/10$ of its maximum value respectively than the effective potential of Johnson and Teller. Thus it is obvious that this change of form has quite an important effect for the values of Δ considered. According to the above estimate, this can be roughly split into two parts: an effective change in radius of approximately 0.05Δ with a corresponding increase in the binding energy of all levels, and a decrease in the slope of the effective potential for the same slope in $V(r)$, by an amount of the order of 0.15Δ . For $\Delta = 3.8 \times 10^{-13}$ cm this is not a negligible

effect. Hence, to achieve the same level sequence, an α of 0.99×10^{13} cm $^{-1}$ ($\Delta \approx 4.45 \times 10^{-13}$ cm) or less would probably be necessary. To obtain the same binding energies with the Duerr equation, the potential depth would have to be decreased by amounts depending on the change in the potential radius. Since this change is a constant, (0.05Δ) , the effective potential depth should have a slight dependence on A .

A final remark should be made about the spin-orbit coupling term predicted by Duerr. This can be rewritten as

$$\frac{870.5}{69} \frac{\hbar^2}{4m_D^2 c^2} \frac{1}{r} \frac{dV(r)}{dr} \sigma \cdot \mathbf{l} = 12.6 \frac{\hbar^2}{4m_D^2 c^2} \frac{1}{r} \frac{dV(r)}{dr} \sigma \cdot \mathbf{l},$$

which differs from the expression we have used not only in magnitude but also in form since the normal mass has been replaced by the effective mass. Unfortunately, this means that it is not accurate to quote a single λ to which Duerr's expression is equivalent because this equivalent λ will vary from level to level. Since the spin-orbit potential is a purely surface effect, a crude estimate can be made by replacing m_D with $\frac{3}{4}m_0$, the effective mass in the region where dV/dr is a maximum. This gives $\lambda = 22.5$, some 60% of the value used in this paper. Actually the equivalent λ will be greater for eigenfunctions which have their last maxima inside the nuclear radius, such as those with only one node. However, the spin-orbit term predicted by Duerr is of the right order of magnitude for the shell model, but it is not clear whether the Duerr formulation is quantitatively sufficient to reproduce the experimental level sequence.

ACKNOWLEDGMENTS

The authors would like to thank Dr. Edward Teller for many interesting discussions and the staff of the UCRL differential analyzer for their cooperation.